Synthetic and Systems Biotechnology 8 (2023) 610–617

Contents lists available at ScienceDirect

Synthetic and Systems Biotechnology

journal homepage: www.keaipublishing.com/en/journals/synthetic-and-systems-biotechnology

Original Research Article

Constructing an artificial short route for cell-free biosynthesis of the phenethylisoquinoline scaffold

Yuhao Zhang, Wan-Qiu Liu, Jian Li *

School of Physical Science and Technology, ShanghaiTech University, Shanghai, 201210, China

ARTICLE INFO

Keywords:
Phenethylisoquinoline scaffold
Artificial pathway
Cell-free biosynthesis
Natural product

ABSTRACT

Plant-originated natural products are important drug sources. However, total biosynthesis of these compounds is often not achievable due to their uncharacterized, lengthy biosynthetic pathways. In nature, phenethylisoquinoline alkaloids (PIAs) such as colchicine are biosynthesized via a common precursor 6,7-dihydroxy-1-(4-hydroxyphenylethyl)-1,2,3,4-tetrahydroisoquinoline (i.e., phenethylisoquinoline scaffold, PIAS). PIAS is naturally synthesized in plants by using two upstream substrates (L-phenylalanine and L-tyrosine) catalyzed by eight enzymes. To shorten this native pathway, here we designed an artificial route to synthesize PIAS with two enzymatic steps from two alternative substrates of 3-(4-hydroxyphenyl) propanol (4-HPP) and dopamine. In the two-step bioconversion, an alcohol dehydrogenase selected from yeast (i.e., ADH7) was able to oxidize its non-native alcohol substrate 4-HPP to form the corresponding aldehyde product, which was then condensed with dopamine by the (*S*)-norcoclaurine synthase (NCS) to synthesize PIAS. After optimization, the final enzymatic reaction system was successfully scaled up by 200 times from 50 μL to 10 mL, generating 5.4 mM of PIAS. We envision that this study will provide an easy and sustainable approach to produce PIAS and thus lay the foundation for large-scale production of PIAS-derived natural products.

1. Introduction

Natural products such as alkaloids are crucial molecules for the treatment of human diseases. The biosynthetic pathways of tetrahydroisoquinoline (THIQ) alkaloids, typically benzylisoquinoline alkaloids (BIAs), have been well studied over the past decades [1]. In contrast, another type of plant-derived THIQ alkaloids - phenethylisoquinoline alkaloids (PIAs) such as colchicine, have just been totally biosynthesized in 2021 [2,3], although the native colchicine producing plant *Colchicum* has been used for the treatment of gout even in the age of classical Greek [4]. In recent years, two PIA-type drugs were approved by the US Food and Drug Administration (FDA) [5,6]. Currently, the main sources to obtain these alkaloids are their native plant producers, despite some of chemical synthesis approaches have been reported [7–9]. Alternatively, enzymatic biotransformation is a powerful tool for natural product synthesis. For example, the pain killer morphine alkaloids have been biosynthesized using the engineered yeast [10]. Tobacco as a plant host has also been used to synthesize alkaloids by reconstitution of their biosynthetic pathways, for instance, the recently reported colchicine biosynthesis in tobacco [2]. However, the product yields of plant-based production systems are normally insufficient for the industrial demand/application.

Previous studies have demonstrated the natural biosynthesis pathways of PIAs, which use L-phenylalanine and L-tyrosine as two precursors [11–13]. While a nearly complete colchicine biosynthetic pathway has been reconstituted in tobacco, the direct enzyme(s) for the synthesis of PIAs scaffold are still missing [2]. This gap might be filled by using (*S*)-norcoclaurine synthase (NCS) - an enzyme involved in the BIAs biosynthetic pathway [14]. Naturally, NCS catalyzes the Pictet-Spengler condensation between dopamine and an aldehyde substrate (e.g., 4-hydroxyphenylacetaldehyde) to form the THIQ scaffold [15]. The reported PIAs scaffold (PIAS) biosynthetic pathway contains a partial lignin pathway, which can convert L-phenylalanine to 4-coumaroyl aldehyde via sequential reactions catalyzed by phenylalanine aminolyase (PAL), cinnamate 4-hydroxylase (C4H), 4-coumarate: coenzyme A ligase (4CL), and cinnamoyl-CoA reductase (CCR) [2]. Then, 4-coumaroyl aldehyde is reduced by a NADPH-dependent double-bond reductase to form 4-hydroxydihydrocinnamoyl aldehyde (4-HDCA),

Peer review under responsibility of KeAi Communications Co., Ltd.
* Corresponding author.
E-mail address: lijian@shanghaitech.edu.cn (J. Li).

https://doi.org/10.1016/j.synbio.2023.09.003
Received 12 July 2023; Received in revised form 1 September 2023; Accepted 15 September 2023
Available online 22 September 2023

which serves as a substrate of the PIAS synthase [14,16]. The other substrate for PIAS synthesis is dopamine, which is derived from L-tyrosine catalyzed by two enzymes in higher plants [2,14]. The native pathway to synthesize PIAS from L-phenylalanine and L-tyrosine consists of eight enzymatic steps (Fig. 1a), which is lengthy and makes reconstitution of the entire pathway in a heterologous host difficult. Thus, designing and constructing a short route to synthesize PIAS is highly desirable.

In this work, we aim to design a short biosynthetic pathway by retrobiosynthesis for the production of PIAS (Fig. 1b). First, the enzyme NCS is selected for the final step enzymatic catalysis, albeit the condensation reaction can be catalyzed by phosphate [17]. This is because that the phosphate-mediated reaction generates racemic products, while NCS exclusively produces the (*S*)-configuration THIQ scaffold [14]. Since the optical activity is essential for the structure of bioactive natural products (e.g., PIAs) [4,18], a phenylpropanal-tolerable NCS is used rather than the phosphate-mediated condensation for precise synthesis [14,17]. Second, to provide the aldehyde substrate for NCS, we intend to use a cheaper alcohol as a precursor, which can be converted to the direct aldehyde substrate by a $NADP^+$-dependent alcohol dehydrogenase (ADH) [19]. However, the common reaction orientation of most ADHs is aldehyde reduction rather than alcohol oxidation [20]. Here, *Saccharomyces cerevisiae* ADH7 is selected because it shows higher activity toward the substrate cinnamyl alcohol compared to other ADHs [21]. Furthermore, previous studies have demonstrated that supplementation of the oxidative coenzyme I and/or II can also reverse the common reaction orientation of ADHs by introducing an oxidase in the enzymatic catalysis system [22–24]. Therefore, a NAD(P)H oxidase (NOX) variant originated from *Streptomyces* is used to regenerate cofactors for ADH7 in our design, because both NADH and NADPH are compatible for this NOX enzyme [23]. Finally, an artificial, short biosynthetic route with a two-step enzymatic cascade for PIAS synthesis is constructed by using three enzymes (i.e., ADH, NOX, and NCS) (Fig. 1b). In this artificial pathway, two precursors of 3-(4-hydroxyphenyl) propanol (4-HPP), which has a similar chemical structure to cinnamyl alcohol, and dopamine are used for PIAS synthesis. After constructing the *in vitro* reaction system, we further optimize the reaction conditions for enhanced PIAS production. Moreover, we scale up the reaction system to demonstrate its feasibility for industrial catalysis and production.

2. Materials and methods

2.1. Chemicals

Dopamine hydrochloride, 3-(4-hydroxyphenyl) propanol (4-HPP), acetonitrile, and formic acid were purchased from Sinopharm Chemical Reagent (Shanghai, China). NADP-Na was purchased from Bidepharm (Shanghai China). Reagents for molecular biology were purchased from Sangon Biotech (Shanghai, China). The standard compounds of 6,7-dihydroxy-1-(4-hydroxyphenylethyl)-1,2,3,4-tetrahydroisoquinoline (i.e., phenethylisoquinoline scaffold, PIAS) and 4-hydroxydihydrocinnamoyl aldehyde (4-HDCA) were the gifts from Dr. Fei Qiao (Tropical Crops Genetic Resources Institute, Chinese Academy of Tropical Agricultural Sciences).

2.2. Construction of plasmids

The genes of *ADH7*, *NOX*, and *NCS* were codon-optimized for *E. coli* and synthesized by GENEWIZ (Suzhou, China). The gene sequences are shown in Table S1. The *ADH7* gene was cloned into the plasmid pET28a, generating pET28a-ADH7. To generate variants of ADH7, all gene fragments (i.e., plasmid backbone, coding sequence, and mutated gene fragments) were amplified by polymerase chain reaction (PCR). Then, the fragments were ligated with the corresponding backbones using the ClonExpress Ultra One Step Cloning Kit (Vazyme). Afterward, the ligated products were transformed into *E. coli* DH5α competent cells, followed by cell growth on LB-agar plates (containing correct concentration of antibiotic) for 12 h. The resulting colonies were selected for further cultivation, plasmid extraction, and DNA sequencing. To generate pPIAS1, the *NCS* and *NOX* genes were inserted into pET28a-ADH7. The resulting plasmid (pPIAS1) contained three genes of

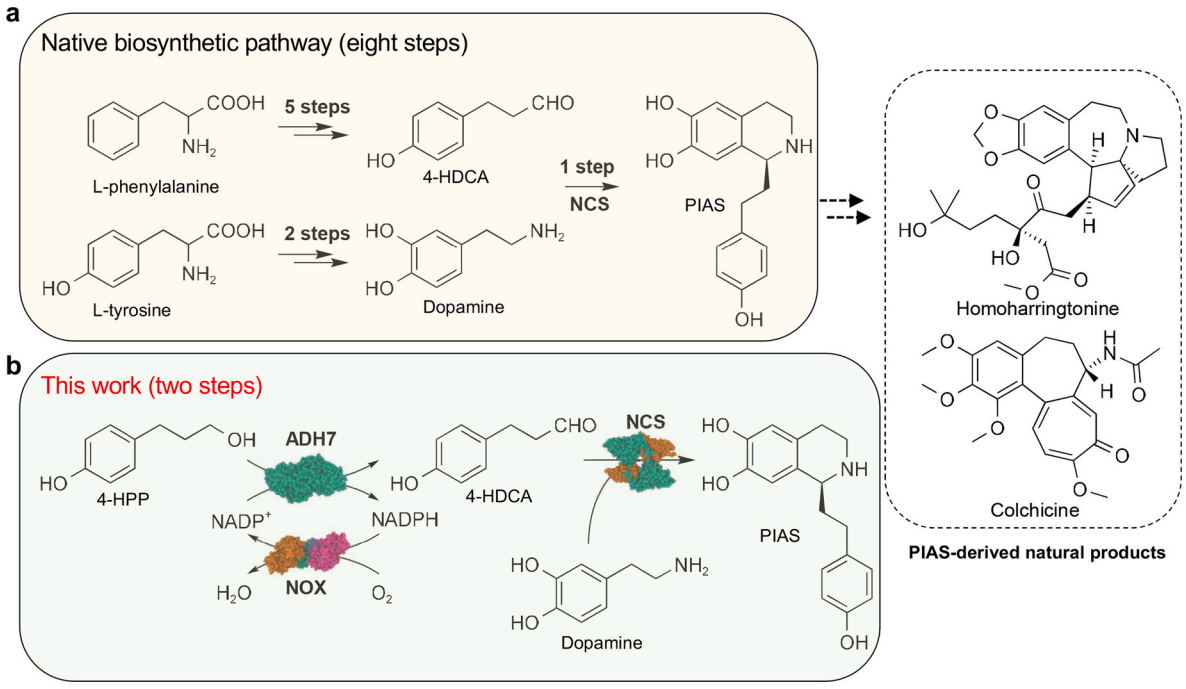

Fig. 1. Biosynthesis of PIAS and the examples of PIAS-derived natural products. (**a**) The native biosynthetic pathway of PIAS with eight enzymatic steps. (**b**) The artificial two-step biosynthesis of PIAS. 4-HPP, 3-(4-hydroxyphenyl) propanol; 4-HDCA, 4-hydroxydihydrocinnamoyl aldehyde; PIAS, phenethylisoquinoline scaffold; ADH7, alcohol dehydrogenase; NOX, NAD(P)H oxidase; NCS, (*S*)-norcoclaurine synthase.

ADH7, *NCS*, and *NOX* (each gene has its own T7 promoter for transcription; see Fig. S1 for the plasmid map). All primers used for PCR amplification are listed in Table S2.

2.3. Cell-free protein synthesis (CFPS) of ADH7 and variants

The cell-free protein synthesis (CFPS) system was reported in our previous studies [25–27]. Briefly, each plasmid was added to the CFPS reaction mixture, containing 12 mM magnesium glutamate, 10 mM ammonium glutamate, 130 mM potassium glutamate, 1.2 mM ATP, 0.8 mM GTP, UTP and CTP, 34 μg/mL folinic acid, 170 μg/mL *E. coli* tRNA mixture, 2 mM each of 20 standard amino acids, 0.33 mM nicotinamide adenine dinucleotide (NAD), 0.27 mM coenzyme A (CoA), 1.5 mM spermidine, 1 mM putrescine, 4 mM sodium oxalate, 33 mM phosphoenolpyruvate (PEP) and 27% (v/v) of cell extracts (prepared from *E. coli* BL21 Star (DE3)). The volume for each CFPS reaction was 15 μL and the incubation was performed at 30 °C for 5 h.

2.4. Preparation of NCS and NOX crude enzyme solutions

E. coli BL21 Star (DE3) harboring the NCS or NOX plasmid was cultivated in liquid LB for 37 °C and 250 rpm. When the OD_{600} reached 0.5, the culture was cooled down to 25 °C and induced with 0.5 mM IPTG. Then, cells were cultivated at 25 °C and 180 rpm for another 5 h. At the end of cultivation, cells were collected by centrifugation at 4000 g and 4 °C for 10 min. Then, cell pellets were washed three times and resuspended with 100 mM Tris-HCl (pH 7.0) buffer (1 mL per gram of wet cell biomass). Next, cells were lysed by sonication (10 s on/off, 50% of amplitude, input energy ~600 J). The lysate was then centrifuged twice at 12,000 g and 4 °C for 10 min. The resultant supernatant (crude enzyme solution) was flash frozen in liquid nitrogen and stored at −80 °C until use.

2.5. Activity assay of NCS, ADH7-NOX, and the ADH7-NOX-NCS cascade

For NCS assay, 5 μL NCS crude enzyme was added to the reaction mixture consisting of 5 mM dopamine, 5 mM 4-HDCA, and 100 mM Tris-HCl buffer (pH 7.0). The total reaction volume was 50 μL. The reaction was incubated at 45 °C for 30 min and quenched by adding 50 μL methanol.

For ADH-NOX assay, 10 μL ADH7-CFPS mixture and 5 μL NOX crude enzyme solution were mixed with 10 mM 4-HPP, 0.5 mM $NADP^+$, 1 mM $ZnSO_4$, and 100 mM Tris-HCl buffer (pH 7.0). The reaction was incubated at 45 °C for 4 h and quenched by adding 50 μL methanol.

For the full cascade reaction (ADH7-NOX-NCS cascade), 5 μL NCS crude enzyme was added to the above ADH7-NOX assay system. The reaction was incubated at 45 °C for 5 h and quenched by adding 50 μL methanol.

2.6. One-pot scale-up reactions

The pPIAS1-harboring *E. coli* strains (BL21 Gold (DE3), BL21 Rosetta (DE3), BL21 (DE3) pLysS, and BL21 Star (DE3)) were cultured in LB medium overnight (50 mg/L kanamycin), respectively. Cell cultivation, collection, and lysis were carried out the same as described above. The reaction volume was scaled up from 50 μL to 1 mL and 10 mL. In each reaction (containing 80% of cell lysates, v/v), 7.5 mM 4-HPP, 7.5 mM dopamine, 0.5 mM $NADP^+$, and 1 mM $ZnSO_4$ were added for the biosynthesis of PIAS. The reaction mixtures were incubated at 45 °C for 5 h, followed by detecting PIAS with LC-MS and HPLC.

2.7. Computational docking

The hydrogen atoms in $NADP^+$ and zinc contained protein model of ADH6 and ADH7 were added by AutoDock Tools. The grid box was selected as center_x = 208.844, center_y = 61.976, center_z = 29.398, size_x = 32, size_y = 36, and size_z = 32. Totally, ten docking results were obtained by UCSF Chimera (www.cgl.ucsf.edu/chimera).

2.8. Analytical methods

The quenched reaction mixtures were centrifuged at 12,000 g for 10 min, and the supernatants were filtered with 0.22 μm nylon membrane before sample loading. 5 μL of each sample was injected into a HPLC system (Thermo Ultimate 3000 UHPLC) with an Agilent Pursuit XRS 5 C_{18} column (4.6 × 250 mm, 5 μm). The column temperature was kept at 30 °C. For analyzing PIAS, the column was eluted with 15% acetonitrile-85% water-0.1% formic acid for 30 min at a flow rate of 0.5 mL/min. For analyzing 4-HPP and 4-HDCA, the column was eluted with 45% acetonitrile-55% water for 20 min at a flow rate of 0.5 mL/min. The compounds were monitored at 280 nm wavelength.

To analyze PIAS by LC-MS, 5 μL of the sample was injected to Agilent 1290 Infinity II with a ZORBAX Original C_{18} column (4.6 × 250 mm, 5 μm). The LC method is the same as described above. The high-resolution mass spectrum analysis is generated in Exactive™ Plus Orbitrap Mass Spectrometer (ThermoFisher Scientific) with an electron spray ionization (ESI). The voltage and capillary temperature are selected as 4 kV and 350 °C, respectively. For positive ion scanning, the mass to charge is selected as 50–750. The sheath, aux, and sweep gas (nitrogen) flow rates are selected as 40, 15, and 15 Arb, respectively. The low-resolution mass/mass spectrum analysis is generated in Angilent 6470 triple quad Mass Spectrometer with an electron spray ionization (ESI). The collision energy is 20 V.

3. Results and discussion

3.1. Enzyme expression and demonstration of their catalytic activity in vitro

To synthesize PIAS from 4-HPP and dopamine, we chose three enzymes to construct a two-step enzymatic cascade reaction (Fig. 1b). First, 4-HPP is oxidized by ADH7 to form the aldehyde substrate (i.e., 4-HDCA), in which NOX is used for regenerating the cofactor ($NADP^+$) for ADH7. In the second step, NCS catalyzes a condensation reaction between 4-HDCA and dopamine to yield PIAS. Prior to building the *in vitro* full pathway, the activity of each enzyme was evaluated. Here, we used different strategies to prepare enzyme samples for the biocatalysis. First, NOX and NCS were expressed *in vivo* using *E. coli* as a host, followed by preparing crude enzyme solutions for the activity assay. The results suggested that both enzymes could be well expressed *in vivo* (Fig. S2a). For the enzyme ADH7, we used an *E. coli*-based cell-free protein synthesis (CFPS) system to express ADH7, which is mainly due to the reason that CFPS has been used for rapid expression and screening enzyme variants without the use of intact living cells [25–27]. Since the catalytic activity of ADH7 toward 4-HPP was not reported previously, here we took advantage of CFPS to rapidly express ADH7 for the initial activity assay. By simply adding the plasmid to CFPS reactions, ADH7 could be successfully expressed at different plasmid concentrations from 0.8 to 4.5 nM (Fig. S2b). When 1.5 or 3 nM of plasmid was used, the expression level of ADH7 was similar, which is higher than the use of 0.8 or 4.5 nM plasmid. Thus, we added 1.5 nM plasmid for cell-free expression of ADH7 in our following experiments.

After confirming the expression of three enzymes, we next sought to determine their catalytic activity, respectively. In the first enzymatic step, we directly used cell-free expressed ADH7 for the catalytic reaction. After ADH7 was expressed in CFPS, the substrate 4-HPP was added to the reaction mixture. Then, the reaction was incubated at 45 °C for 4 h, followed by HPLC analysis to detect the product of 4-HDCA. However, the detection of 4-HDCA in the ADH7 reaction without NOX was not obvious, although trace amount of 4-HDCA could be detected (Fig. 2a, middle). This is likely due to the lack of sufficient cofactor ($NADP^+$) or

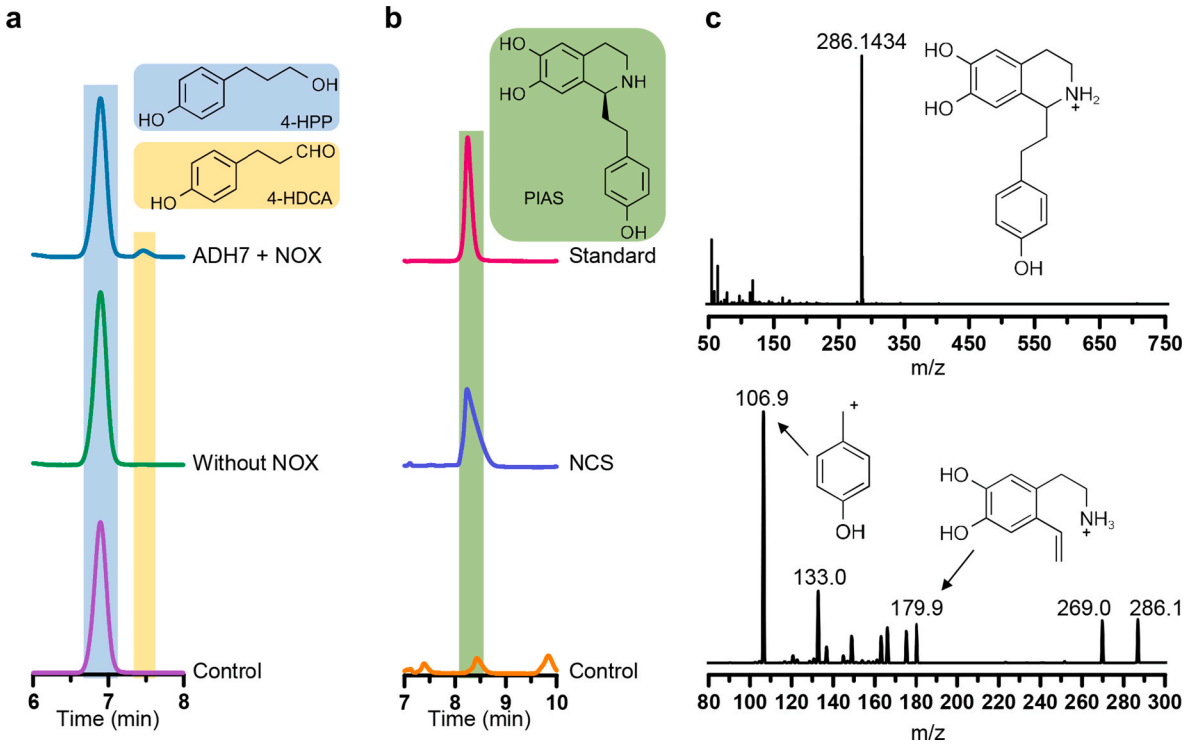

Fig. 2. Detection of the target compounds generated by the enzymatic reactions. (**a**) HPLC analysis of the substrate (4-HPP) and the intermediate (4-HDCA) from the ADH7-NOX catalyzed reactions. (**b**) HPLC analysis of the product (PIAS) from the NCS catalyzed reactions. (**c**) LC-MS detection of PIAS. Top, MS spectrum of PIAS; Bottom, MS/MS spectrum of PIAS with representative fragment ions. The control reactions were performed by mixing cell extract and CFPS reaction without enzymes.

$NADP^+$ could not be regenerated to support the ADH7-catalyzed oxidation of 4-HPP. When NOX was supplemented to the ADH7 reaction, the formation of 4-HDCA was notably enhanced (Fig. 2a, top) as compared to the group without NOX. Our results suggested that with the aid of NOX for cofactor regeneration ADH7 favors the reaction of alcohol oxidation rather than aldehyde reduction. As a result, selecting ADH7 to synthesize 4-HDCA is feasible to construct the full artificial biosynthetic route (Fig. 1b). Then, we added 4-HDCA and dopamine as two substrates to the NCS-based *in vitro* reaction. The results showed that NCS was active to synthesize PIAS with the two substates (Fig. 2b, middle and 2c). In addition, we also observed the synthesis of PIAS in the control reaction without the presence of NCS (Fig. 2b, bottom), which is due to the spontaneous, non-enzymatic condensation between the two substrates [17,28]. However, this background synthesis is notably lower than the product synthesized by NCS (Fig. 2b, middle and bottom). Overall, three enzymes selected in this artificial route are active for PIAS biosynthesis.

3.2. Generation of ADH7 variants

Although ADH7 is active to convert 4-HPP to 4-HDCA, the activity of ADH7 toward the non-natural substrate was relatively low (Fig. 2a). To increase its catalytic activity, we tried to engineer ADH7 by modifying several key amino acid residues around the activity center. In *S. cerevisiae*, another alcohol dehydrogenase (ADH6) is an isoenzyme of ADH7 and shows 64% amino acid sequence identity to ADH7 [21,29]. Both enzymes belong to the cinnamoyl alcohol dehydrogenase family and have the same optimum aldehyde substrate (cinnamaldehyde) [21,29]. However, the catalytic efficiency toward the oxidation of cinnamoyl alcohol is much higher (20-fold) for ADH7 than for ADH6 [21,29]. Since the structure of ADH6 has been solved (PDB ID: 1PIW), it was used as a template to predict the structure model of ADH7 by SWISS-MODEL (Fig. 3a and b). Then, the substrate (i.e., cinnamoyl alcohol and 4-HPP) binding models with the two enzymes were simulated by AutoDock Vina, respectively (Fig. 3c and d). The molecular docking results indicated that the residues D117, V119, A278, and M293 of ADH7 locate in the substrate binding site (Fig. 3d), but they are different from ADH6 (Fig. 3c). This suggests that these residues in ADH6/ADH7 might influence the binding of 4-HPP or other substrates such as cinnamoyl alcohol. Thus, these residues were selected to make single site mutation, yet not with a saturation mutation strategy. Instead, we chose several potential amino acids trying to enhance the performance of ADH7. For example, three variants were generated to mutate the position M293, because these mutations (M293Y, M293F, and M293K) might improve the π-π stack with the aromatic ring of 4-HPP (Y and F) and the binding with the phenol hydroxy group (K). However, our CFPS expression and activity assay indicated that while the ADH7 variants were well expressed, their catalytic activity was comparable to the wild-type ADH7 without obvious increase (Fig. S3). As a result, the wild-type ADH7 was used in the subsequent experiments to optimize the biosynthetic route for enhanced production of PIAS.

3.3. Effect of key physicochemical factors on the enzymatic reactions

Having demonstrated the catalytic activity of the selected enzymes, we next wanted to evaluate the effect of different key parameters on the enzymatic reactions. First, we tried to increase the conversion of 4-HPP to 4-HDCA catalyzed by ADH7. Since the cofactor $NADP^+$ was important for the ADH7 activity, different concentrations of $NADP^+$ were added to the reactions. The results suggested that 0.5 mM $NADP^+$ was able to support the enzymatic reaction with a relative activity of 86% in the group of ADH7+NOX, which is about 3.7 times higher than the control group (ADH alone in the reaction) (Fig. 4a). Although the enzyme activity was increased by adding more $NADP^+$ (5 mM), the improvement was not significant and, thus, 0.5 mM $NADP^+$ was used in the following reactions. Next, we tested the effect of reaction temperature, ranging from 25 °C to 60 °C, on the ADH7 catalysis. We observed that the

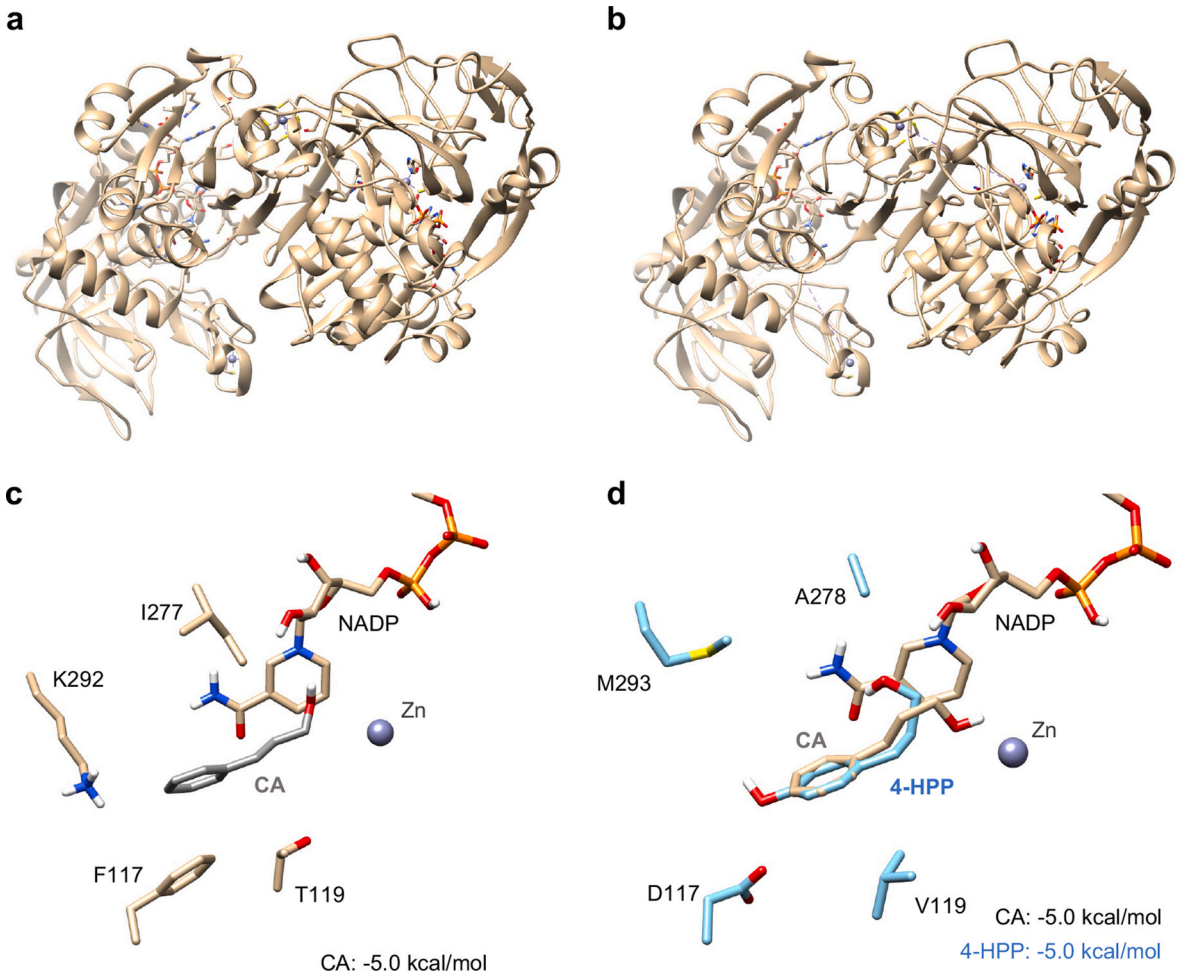

Fig. 3. The predicted protein structure of ADH7 and comparison of substrate recognition sites. (**a**) The protein structure of ADH6 (PDB ID: 1PIW). (**b**) Homology model of ADH7 constructed by SWISS-MODEL using ADH6 as a template (64% identity). (**c**) Molecular docking of ADH6 with the substrate CA. (**d**) Molecular docking of ADH7 with the substrates CA and 4-HPP. CA, cinnamoyl alcohol; 4-HPP, 3-(4-hydroxyphenyl) propanol.

enzyme activity was gradually improved by increasing the temperature from 25 °C to 45 °C and the highest activity reached at 45 °C (Fig. 4b). Further increase of the temperature to 60 °C led to a sharp decrease of the activity, which is likely ascribed to the denaturation of the enzyme at a high temperature. Our observation is in agreement with the reported optimum temperature range of the enzyme NCS (40–55 °C) [15,30]. Therefore, the two step enzymatic reactions were then performed at 45 °C. Next, we varied the concentration of the substrate 4-HPP added to the reaction mixture. We found that increasing the 4-HPP concentration from 5 mM to 7.5 mM yielded a 4.5-fold improvement of the enzyme activity (Fig. 4c). Although 10 mM 4-HPP further gave rise to a slightly higher (8%) ADH7 activity than that of 7.5 mM 4-HPP, we finally used 7.5 mM 4-HPP as a suitable substrate concentration for the cascade reaction. This is because the activity of the second step enzyme NCS was slightly inhibited with 10 mM 4-HPP (Fig. S4). The reason is likely due to the similarity of the chemical structures between 4-HPP and 4-HDCA, which might compete to bind the active site of NCS. In addition, we observed that the ADH7-catalyzed reaction terminated after about 4–6 h incubation (Fig. 4d). Finally, we investigated the second step reaction catalyzed by NCS. As reported previously, the non-enzymatic condensation of 4-HDCA and dopamine could occur to form PIAS [17,28]. This was also observed in our experiments (Fig. 2b, bottom). Therefore, we compared two reaction groups, including ADH7+NOX and ADH7+NOX + NCS (the complete cascade reaction). The PIAS concentrations were calculated according to a calibration curve prepared with a standard compound (Fig. S5). Clearly, the final concentration of PIAS reached 3.4 mM with NCS after 5 h reaction, which is over 5 times higher than that of the reaction without NCS (Fig. 4e). This suggests that NCS is highly active to execute the catalysis, and the two-step cascade reaction can be terminated at 5 h with a high PIAS yield (Fig. 4d and e). Interestingly, when the two step enzymatic reactions were coupled, 45.3% of 4-HPP (7.5 mM) could be converted to the final product PISA (3.4 mM), suggesting that the catalytic efficiency of wild-type ADH7 in the artificial pathway was sufficient to support PISA synthesis. In addition, the concentration of dopamine in the reaction was also evaluated and the result showed that 7.5 mM dopamine was suitable for the high product formation (Fig. 4f).

3.4. *Preparing highly active enzyme-enriched cell lysates for scale-up production*

Next, we sought to scale up the reaction system for PIAS production. To this end, we first optimized the conditions for cell cultivation, enzyme expression, and cell lysis. To coexpress three enzymes (i.e., ADH7, NOX, and NCS), we constructed a plasmid by inserting the related three genes – each with its own T7 promoter – into the backbone vector pET28a, generating the expression plasmid pPIAS1 (see Fig. S1 for the map). Then, pPIAS1 was transformed into four different *E. coli* strains for enzyme expression, including BL21 Gold (DE3), BL21 Rosetta (DE3), BL21 (DE3) pLysS, and BL21 Star (DE3). Coexpression of the three enzymes was verified by the Western-blot analysis (Fig. S2c). After cultivation, cells were lysed and the lysates (supernatants) were used for

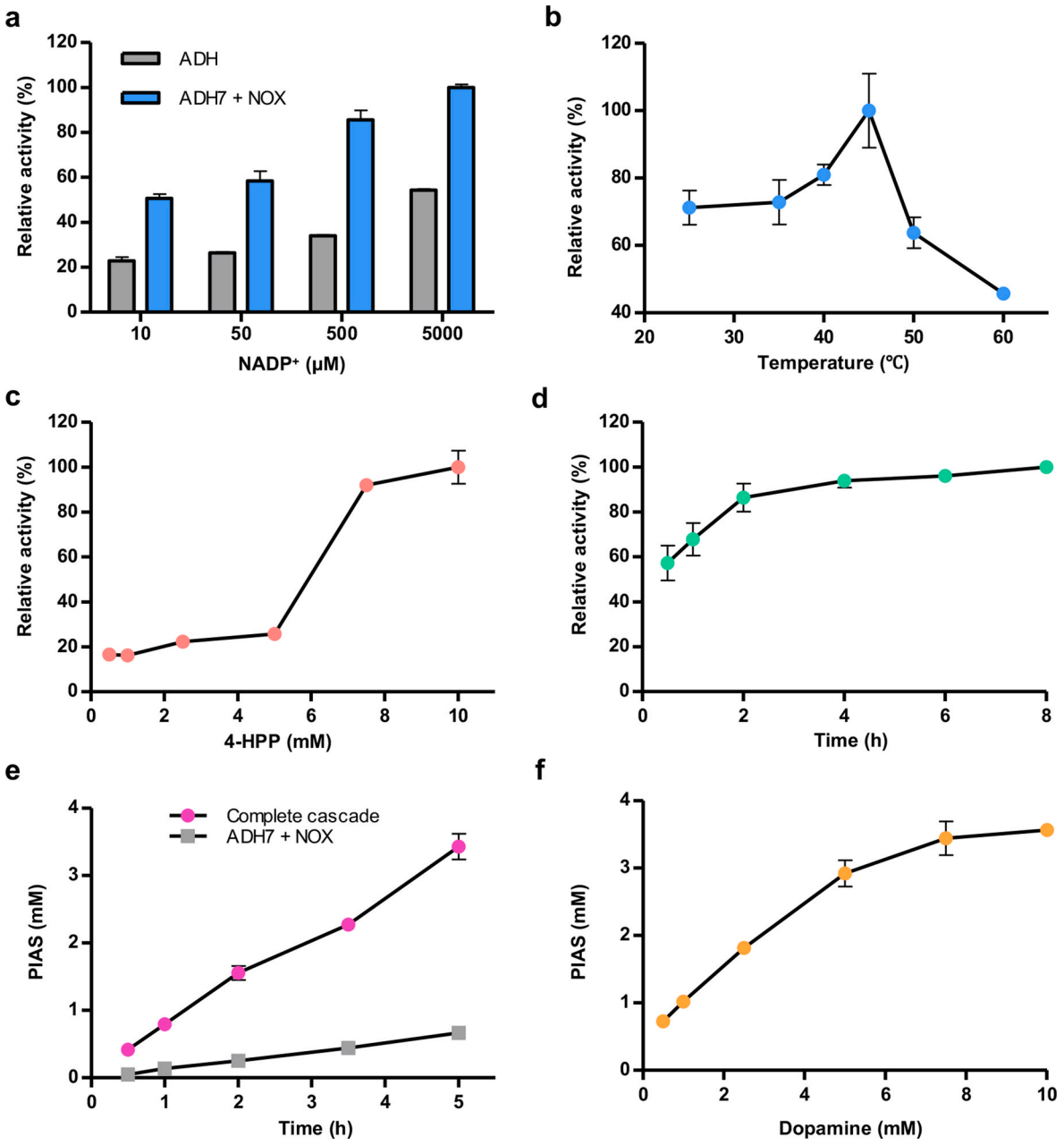

Fig. 4. Evaluation of different factors on the two-step enzymatic reactions. Effect of (**a**) $NADP^+$ concentration, (**b**) reaction temperature, (**c**) substrate (4-HPP) concentration, and (**d**) reaction time on the ADH7-based enzymatic reaction (the reactions were supplemented with NOX for regeneration of the cofactors $NADP^+$/NADPH). In the reactions (**a**)–(**d**), a standard reaction (50 μL) contains the following components: 10 μL ADH7-CFPS mixture, 5 μL NOX crude enzyme solution, 10 mM 4-HPP, 0.5 mM $NADP^+$, 1 mM $ZnSO_4$, and 100 mM Tris-HCl buffer (pH 7.0). The reaction was incubated at 45 °C for 4 h and quenched by adding 50 μL methanol. (**e**) Construction of the complete two-step cascade reaction for PIAS synthesis. (**f**) Effect of the substrate (dopamine) concentration on PIAS formation. In the reactions (**e**)–(**f**), a standard reaction (50 μL) contains the following components: 10 μL ADH7-CFPS mixture, 5 μL NOX crude enzyme solution, 5 μL NCS crude enzyme solution, 7.5 mM 4-HPP, 5 mM dopamine, 0.5 mM $NADP^+$, 1 mM $ZnSO_4$, and 100 mM Tris-HCl buffer (pH 7.0). The reaction was incubated at 45 °C for 5 h and quenched by adding 50 μL methanol. Values show means with error bars representing standard deviations (s.d.) of at least three independent experiments.

biocatalytic reactions. As shown in Fig. 5a, cell lysates prepared from BL21 Gold (DE3) performed the best, giving rise to more than 1 mM of PIAS, which is 17% higher than the second group of BL21 (DE3) pLysS. Using the *E. coli* BL21 Gold (DE3) strain, we then investigated the effect of enzyme expression temperature and IPTG concentration on the PIAS production. The results indicated that the optimum temperature and IPTG concentration for cell cultivation and enzyme expression were 25 °C and 100 μM (Fig. 5b and c), respectively. Cells were lysed by sonication and thus the input energy was optimized. We found that a relatively low energy between 250 and 750 J was sufficient to generate highly active cell lysates, yet further increasing the input energy (>1000 J) significantly reduced the PIAS yield (Fig. 5d). In addition, we evaluated the cell cultivation time on PIAS synthesis. After induction with 100 μM IPTG, cells were further incubated at 25 °C for a total of 48 h. During the cultivation, cells were collected at different time points for wet weight measurement. At each point, cells were also lysed to perform biocatalysis. The results showed that cells could keep growing over 48 h; however, the highest PIAS yield was achieved at 12 h cultivation (Fig. 5e).

Finally, we gradually scaled up the reaction volume from 50 μL to 1 mL and 10 mL. The 1 mL and 10 mL reactions were carried out in 15 mL tubes and 50 mL flasks, respectively. The results indicated that with the

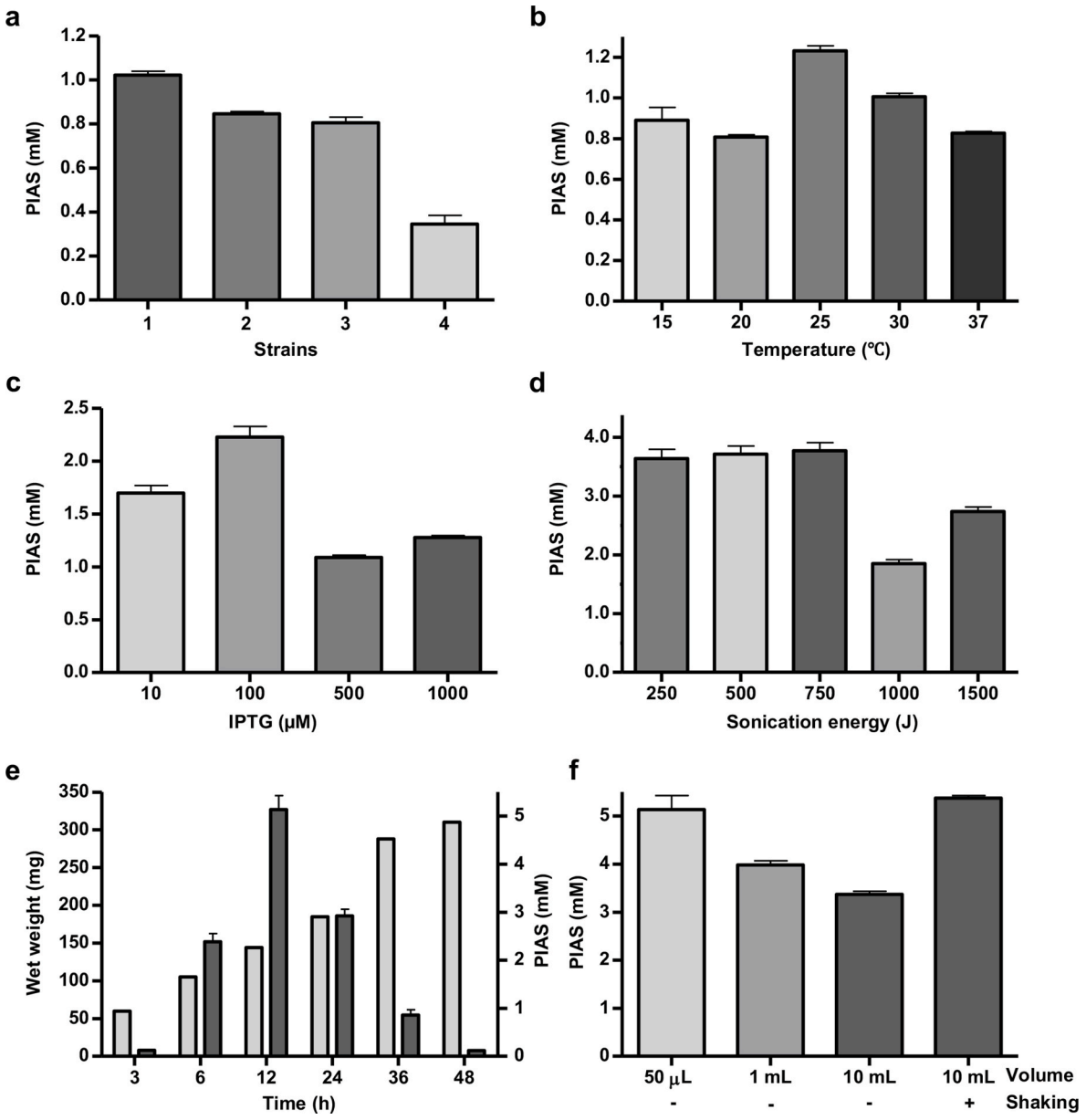

Fig. 5. Optimization and scale-up production of PIAS. (**a**) The selection of different *E. coli* strains to coexpress three enzymes (i.e., ADH7, NOX, and NCS) for PIAS synthesis. 1, *E. coli* BL21 Gold (DE3); 2, *E. coli* BL21 (DE3) pLysS; 3, *E. coli* BL21 Rosetta (DE3); 4, *E. coli* BL21 Star (DE3). Effect of (**b**) enzyme expression temperature, (**c**) IPTG concentration, and (**d**) sonication energy on the production of PIAS. (**e**) PIAS biosynthesis using different cell lysates prepared from cultivations between 3 and 48 h. Cell wet weights were measured by collecting cells at different time points (light gray). PIAS concentrations were shown in dark gray columns. (**f**) Scale-up production of PIAS. The shaking reaction was performed at 220 rpm. In the reactions (**a**)–(**f**), a standard reaction (50 μL) contains the following components: 40 μL cell lysates (consisting of ADH7, NOX, and NCS), 7.5 mM 4-HPP, 7.5 mM dopamine, 0.5 mM $NADP^+$, 1 mM $ZnSO_4$, and 100 mM Tris-HCl buffer (pH 7.0). The reaction was incubated at 45 °C for 5 h and quenched by adding 50 μL methanol. Values show means with error bars representing standard deviations (s.d.) of at least three independent experiments.

increase of reaction volume the PIAS yield reduced 34% from 50 μL to 10 mL reactions (Fig. 5f). This is probably due to the lack of dissolved oxygen, which is required by the enzyme NOX (Fig. 1b), in the large volume of reaction mixture. To supply sufficient oxygen for NOX, we then incubated the 10 mL reaction with shaking at 220 rpm. By doing this, the synthesis of PIAS was significantly enhanced as compared to the 10 mL reaction without shaking, reaching the highest PIAS yield of 5.4 mM (Fig. 5f). Overall, our work provides a feasible approach for PIAS synthesis that holds the potential for large-scale production in the future.

4. Conclusions

In this study, we demonstrated the construction of an artificial short pathway for the biosynthesis of PIAS, an important precursor of phenethylisoquinoline alkaloids. Three enzymes were employed to perform a two-step cascade reaction to synthesize PIAS, avoiding the use of the long native biosynthetic pathway with eight enzymatic steps [31]. In particular, the ADH7 from *S. cerevisiae* was selected to oxidize the alcohol substrate (4-HPP) to form the aldehyde product (4-HDCA) with the help of the enzyme NOX. The condensation of 4-HDCA and dopamine was catalyzed by NCS, yielding PIAS. The activity of each enzyme was first confirmed and then three enzymes were mixed to construct the full biosynthetic pathway. After optimization, the enzymatic reaction

system was scaled up from 50 μL to 10 mL, which finally produced 5.4 mM of PIAS. To the best of our knowledge, this is the first report to synthesize PIAS in two steps by combining three enzymes (ADH7, NOX, and NCS). Looking forward, our work will offer an easy, green, and sustainable approach to produce PIAS and, therefore, pave the way for large-scale production of PIAS-derived natural products such as the clinical drug colchicine.

CRediT authorship contribution statement

Yuhao Zhang: Investigation, Methodology, Visualization, Writing – original draft. **Wan-Qiu Liu:** Investigation, Methodology. **Jian Li:** Conceptualization, Supervision, Funding acquisition, Resources, Writing – review & editing.

Declaration of competing interest

The authors declare that they have no known competing financial interests or personal relationships that could have appeared to influence the work reported in this paper.

Acknowledgements

This work was supported by grants from the National Natural Science Foundation of China (32171427 and 31971348). We also acknowledged Dr. Fei Qiao (Tropical Crops Genetic Resources Institute, Chinese Academy of Tropical Agricultural Sciences) for generously providing us the standard compounds of phenethylisoquinoline scaffold (PIAS) and 4-hydroxydihydrocinnamoyl aldehyde (4-HDCA).

Appendix A. Supplementary data

Supplementary data to this article can be found online at https://doi.org/10.1016/j.synbio.2023.09.003.

References

[1] Beaudoin GAW, Facchini PJ. Benzylisoquinoline alkaloid biosynthesis in opium poppy. Planta 2014;240:19–32.
[2] Nett RS, Lau W, Sattely ES. Discovery and engineering of colchicine alkaloid biosynthesis. Nature 2020;584:148–53.
[3] Nett RS, Sattely ES. Total biosynthesis of the tubulin-binding alkaloid colchicine. J Am Chem Soc 2021;143:19454–65.
[4] Larsson S, Ronsted N. Reviewing colchicaceae alkaloids – perspectives of evolution on medicinal chemistry. Curr Top Med Chem 2013;14:274–89.
[5] Jalil Miah MA, Hudlicky T, Reed JW. In the alkaloids: chemistry and biology, vol. 51. Elsevier; 1998. p. 199–269.
[6] Yang LPH. Oral colchicine (Colcrys®) in the treatment and prophylaxis of gout. Drugs 2010;11:1603–13.
[7] Graening T, Schmalz HG. Total syntheses of colchicine in comparison: a journey through 50 Years of synthetic organic chemistry. Angew Chem Int Ed 2004;43:3230–56.
[8] Reed JW, Hudlicky T. The quest for a practical synthesis of morphine alkaloids and their derivatives by chemoenzymatic methods. Acc Chem Res 2015;48:674–87.
[9] Zhang ZW, Zhang XF, Feng JY, Yang H, Wang CC, Feng JC, Liu S. Formal synthesis of cephalotaxine. J Org Chem 2013;78:786–90.
[10] Galanie S, Thodey K, Trenchard IJ, Interrante MF, Smolke CD. Complete biosynthesis of opioids in yeast. Science 2015;349:1095–100.
[11] Herbert RB, Knagg E. The biosynthesis of the phenethylisoquinoline alkaloid, colchicine,from cinnamaldehyde and dihydrocinnamaldehyde. Tetrahedron Lett 1986;27:1099–102.
[12] Nett RS, Guan X, Smith K, Faust AM, Sattely ES, Fischer CR. D_2O Labeling to measure active biosynthesis of natural products in medicinal plants. AIChE J 2018;64:4319–30.
[13] Sivakumar GK, Krishnamurthy V, Hao J, Paek KY. Colchicine production in Gloriosa superba calluses by feeding precursors. Chem Nat Compd 2004;40:499–502.
[14] Nishihachijo M, Hirai Y, Kawano S, Nishiyama A, Minami H, Katayama T, Yasohara Y, Sato F, Kumagai H. Asymmetric synthesis of tetrahydroisoquinolines by enzymatic Pictet–Spengler reaction. Biosci Biotechnol Biochem 2014;78:701–7.
[15] Samanani N, Facchini PJ. Isolation and partial characterization of norcoclaurine synthase, the first committed step in benzylisoquinoline alkaloid biosynthesis, from opium poppy. Planta 2001;213:898–906.
[16] Youn B, Kim SJ, Moinuddin SGA, Lee C, Bedgar DL, Harper AR, Davin LB, Lewis NG, Kang C. Mechanistic and structural studies of apoform, binary, and ternary complexes of the arabidopsis alkenal double bond reductase At5g16970. J Biol Chem 2006;281:40076–88.
[17] Pesnot T, Gershater MC, Ward JM, Hailes HC. Phosphate mediated biomimetic synthesis of tetrahydroisoquinoline alkaloids. Chem Commun 2011;47:3242–4.
[18] Pérard-Viret J, Quteishat L, Alsalim R, Royer J, Dumas F. In the alkaloids: chemistry and biology, vol. 78. Elsevier; 2017. p. 205–352.
[19] Cederbaum AI. Alcohol metabolism. Clin Liver Dis 2012;16:667–85.
[20] Uthoff S, Steinbüchel A. Purification and characterization of an NAD^+-Dependent XylB-like aryl alcohol dehydrogenase identified in acinetobacter baylyi ADP1. Appl Environ Microbiol 2012;78:8743–52.
[21] Larroy C, Parés X, Biosca JA. Characterization of a Saccharomyces cerevisiae NADP(H)-dependent alcohol dehydrogenase (ADHVII), a member of the cinnamyl alcohol dehydrogenase family. Eur J Biochem 2002;269:5738–45.
[22] Bartsch S, Brummund J, Köpke S, Straatman H, Vogel A, Schürmann M. Optimization of alcohol dehydrogenase for industrial scale oxidation of lactols. Biotechnol J 2020;15:2000171.
[23] Petschacher B, Staunig N, Müller M, Schürmann M, Mink D, De Wildeman S, Gruber K, Glieder A. Cofactor specificity engineering of Streptococcus mutans NADH oxidase 2 for $NAD(P)^+$ regeneration in biocatalytic oxidations. Comput Struct Biotechnol J 2014;9:e201402005.
[24] Aalbers FS, Fraaije MW. Design of artificial alcohol oxidases: alcohol dehydrogenase–NADPH oxidase fusions for continuous oxidations. Chembiochem 2019;20:51–6.
[25] Tian X, Liu WQ, Xu H, Ji X, Liu Y, Li J. Cell-free expression of NO synthase and P450 enzyme for the biosynthesis of an unnatural amino acid L-4-nitrotryptophan. Synth. Syst. Biotechnol. 2022;7:775–83.
[26] Liu WQ, Wu C, Jewett MC, Li J. Cell-free protein synthesis enables one-pot cascade biotransformation in an aqueous-organic biphasic system. Biotechnol Bioeng 2020;117:4001–8.
[27] Chen Y, Liu WQ, Zheng X, Liu Y, Ling S, Li J. Cell-free biosynthesis of lysine-derived unnatural amino acids with chloro, alkene, and alkyne groups. ACS Synth Biol 2023;12:1349–57.
[28] Bonamore A, Rovardi I, Gasparrini F, Baiocco P, Barba M, Molinaro C, Botta B, Boffi A, Macone A. An enzymatic, stereoselective synthesis of (S)-norcoclaurine. Green Chem 2010;12:1623–7.
[29] Larroy C, Ferna MR, Gonza E, Pare X, Biosca JA. Characterization of the Saccharomyces cerevisiae YMR318C (ADH6) gene product as a broad specificity NADPH-dependent alcohol dehydrogenase: relevance in aldehyde reduction. Biochem J 2002;361:163–72.
[30] Samanani N, Liscombe DK, Facchini PJ. Molecular cloning and characterization of norcoclaurine synthase, an enzyme catalyzing the first committed step in benzylisoquinoline alkaloid biosynthesis. Plant J 2004;40:302–13.
[31] Qiao F, He YD, Zhang YH, Jiang XF, Cong HQ, Wang ZM, Sun HP, Xiao YB, Zhao YC, Nick P. Elucidation of the 1-phenethylisoquinoline pathway from an endemic conifer Cephalotaxus hainanensis. Proc Natl Acad Sci USA 2023;120:e2209339120.